ChemTech

International Journal of ChemTech Research
CODEN (USA): IJCRGG, ISSN: 0974-4290, ISSN(Online):2455-9555
Vol.9 No.12, pp 791-798, 2016

Structural, Optical and Electrical Properties for NiO Thin Films Prepared by Pulsed Laser Deposition

Wajeha A. Zoba

University of Babylon, College of science for women, Department of physics, Babylon -Iraq

Abstract : Asimple,inexpensive,pulsed laser deposition(PLD)technique used to deposite nickel oxide NiO thin films on glass substrate. Structural, optical and electricalparameters were studied. Moreover, the surface morphology of the deposited samples was also examined. The optical absorbance spectra for the studied samples showed the maximum value around 280 nm.On the other hand, thickness interferometry measurement of the tested samples was around 400 nm. The optical energy gap and refractive index of the NiO thin film was determined. Electrical measurement showed that the film was P-type.
Keywords:Nickel oxidethin films, pulsed laser deposition (PLD) technique.

Introduction

Nickel oxide (NiO) is the most exhaustively investigated transition metal oxide. It is a NaCltype antiferromagnetic oxide semiconductor. It offers promising candidature for many applications such as solar thermal absorber[1],catalyst forO2 evolution[2], photoelectrolysis[3] and electrochromic device[4]. NiO is also a well-studied material as the positive electrode in batteries[5]. Pure stoichiometric NiO crystals are perfect insulators[6]. Several efforts have been made to explain the insulating behavior of NiO. Appreciable conductivity can be achieved in NiO by creating Ni vacancies or substituting Li for Ni at Ni sites[6].NiO thin films have been prepared by various techniques that involve: vacuum evaporation[7], electron beam evaporation[8], Rf–magnetron sputtering[9,10], anodic oxidation[11], chemical deposition[12,13], atomic layer epitaxy[14], sol–gel[15] and spray pyrolysis technique (SPT)[16].Pulsed laser deposition (PLD) is a very important and powerful technique for the growth of thin films of complex materials. It consists of three major parts, laser, vacuum system and chamber[17].

2.Experimental procedure

The pulsed laser deposition experiment is carried out inside a vacuum chamber generally at (10-3 Torr) vacuum conditions, at low pressure of a background gas for specific cases of oxides and nitrides. Photograph of the set-up of laser deposition chamber, as shown in Figure (1), which shows the arrangement of the system include the target and substrate holders inside the chamber with respect to the laser beam. The focused Nd:YAG SHG Q-switching laser beam coming through a window is incident on the target surface making an angle of 45° with it. The substrate is placed in front of the target with its surface parallel to that of the target. Sufficient gap is kept between the target and the substrate so that the substrate holder does not obstruct the incident laser beam. Modification of the deposition technique is done by many investigators from time to time with the aim of obtaining better quality films by this process. These include rotation of the target, heating the substrate, positioning of the substrate with respect to target.

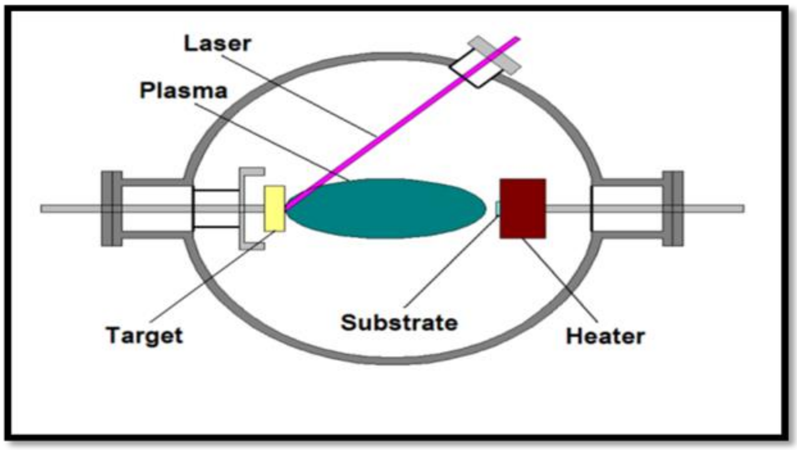

Figure 1: Schematic diagram of PLD system [18].

3.Result and discussion

3.1 Structural properties

The thickness of the deposited sample was estimated to be around 400 nm using Tolansky method**.**Figure(2)illustrates a photo of the interference fringes pattern obtained for one of the samples.

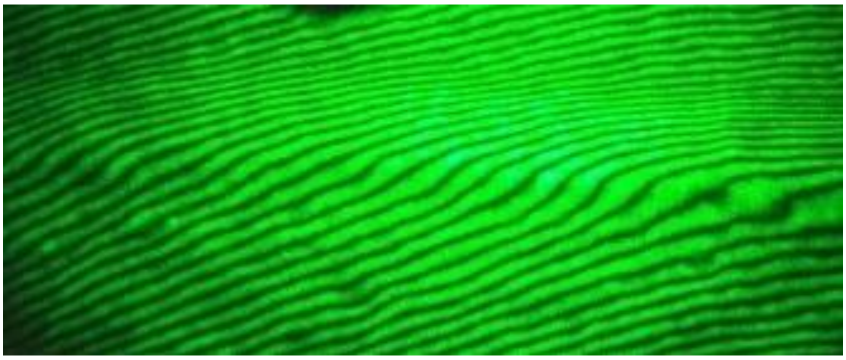

Figure 2: NiO thickness measurement via the interference Tolansky method

X-ray diffraction investigates the structural type of the NiO thin films prepared by PLD. The XRD pattern for films deposited at 400 ^{0}Cshowed that they have a polycrystalline structure after annealing at 450 ^{o}C for three hours and amorphous structure before annealing,as presented in Figure(3).Moreover, the peaks of XRD indicate a cubic phase structure for NiO thin films. Figure (3) also shows that the intensity of the (100) , (111) and (200) peaks increased with increasing the annealing temperature.Table 1, gives the essential XRD data which include the FWHM and the (hkl) of the main diffraction peaks. Also evaluated are the grain sizes using the well-knownScherer'sformula[19] as given below:

$G = 0.94\ \lambda / \beta \cos\theta$ …..…. (1)

Where G is the average crystalline grain size(mean crystalline size), λ is the wavelength (1.5406Å), β represents the full-width at half maximum (FWHM) of the peak in radian and θ is the Bragg's diffraction angle of the XRD peak in degree. The calculated values of grain size for NiO thin film were found to vary between 16.1–20.2 nm at different planes.

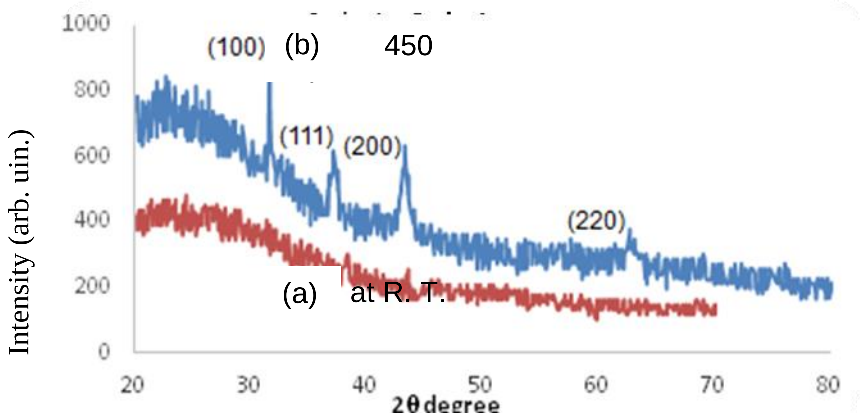

Figure 3: XRD pattern of NiO thin film (a)before annealing and (b) after annealing at 450 °C.

Table 1: Diffraction data for the NiO electrostatically – sprayed samples.

Peak No.	2 Theta (deg)	(hkl)	G (nm)
1	33	100	20.2
2	37	111	20.2
3	44	200	19.5
4	64	220	16.1

3.2 Thin film surface characterization

Figure (4)provides an SEM photo showing the grains of the NiO thin film. Shows that the film is homogeneously distributed for pure NiO.

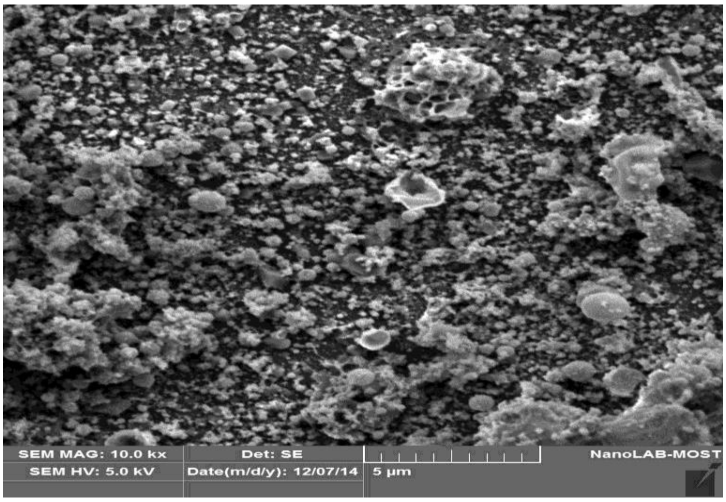

Figure4:SEM photo showing sub- micrometer grain size of the NiO thin film.

3.3 Atomic Force Microscopy (AFM)

For the purpose of examining the NiO thin film, Atomic Force Microscope (AFM) tests were devoted to examine the deposited film homogeneity, surface roughness, and morphology. For many studies, AFM was applied together with another optical characterization or morphological technique.The surface roughness of the thin films is an important parameter which besides describing the light scattering at the surface gives a significant indication about the quality of the surface under investigation. The increase in surface roughness of the films, therefore, it is very important to investigate the surface morphology of the films. 2D and 3D AFM image of NiO thin films are shown in figure (5). It shows that the morphology of the NiO thin films has larger intensity of grain size, which indicates the crystalline nature of the films is of high crystallinity and good surface morphology. It is known that the granular thin films show higher surface area.

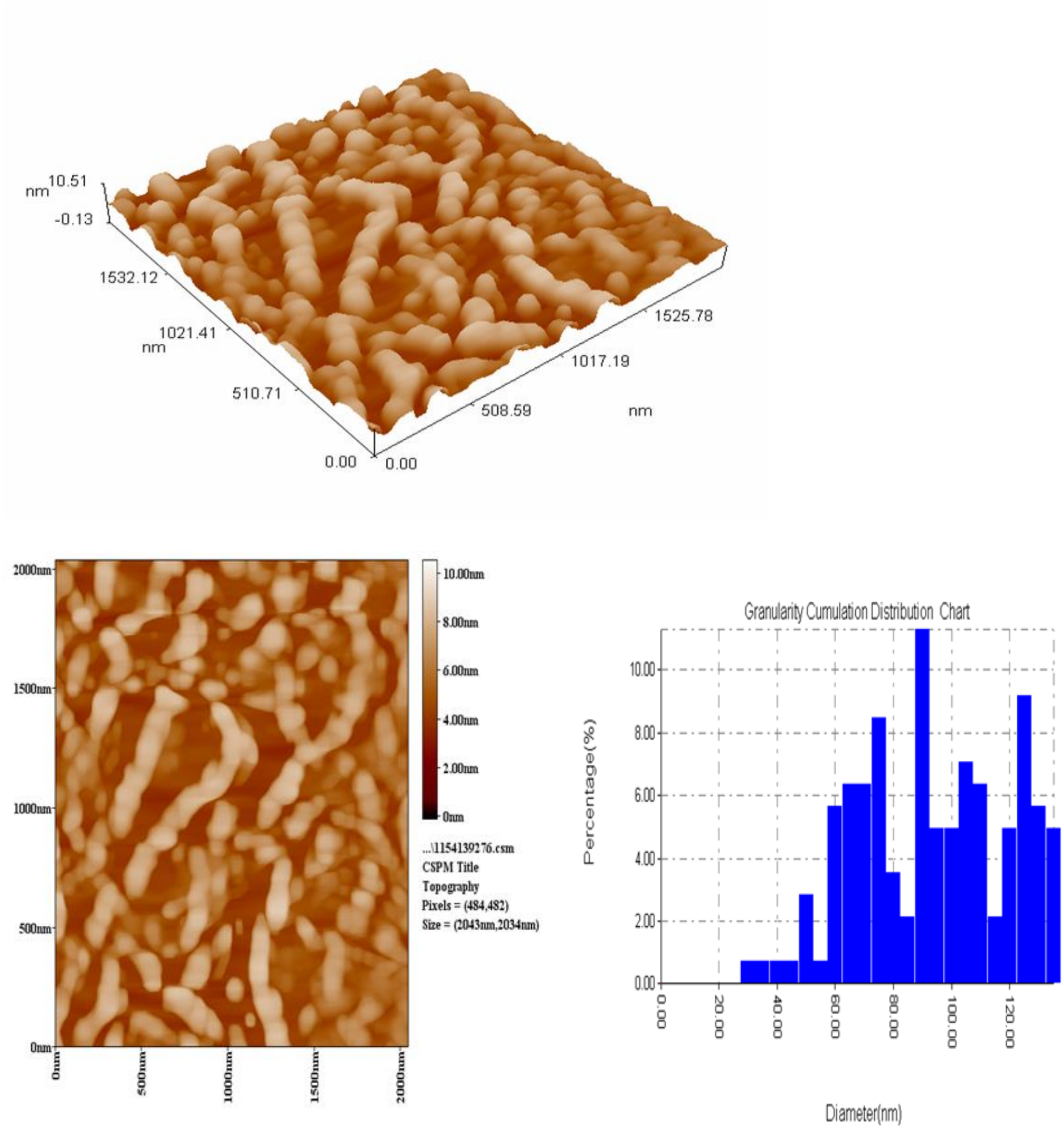

Figure 5: 3D and 2D AFM image for pure NiO thin films.

3.4 Optical and electrical properties of thin films.

The optical characteristics which involve the optical energy gap Eg, and the optical constants (i.e.refractive index n, extinction coefficient k, real dielectric constantƐrand imaginary dielectric Ɛi), were studied within the range (200-1000)nm for NiO thin films deposited by PLD technique. The absorbance spectrum, shown in Figure (6) is a high band gap semiconductor with the absorption edge in the UV region and no absorption edge in the visible region. Recorded optical data were further analyzed to calculate the band gap energy of the NiO films using classical relation.Figure(7) shows the variation of $(\alpha h\upsilon)^2$ as a function of incident photon energy (hυ) for NiO thin films. It can be observed from this Figure that the energy gap equal to 3.5 eV as estimated from the extrapolation of the linear part of the spectrum to $(\alpha h\upsilon)^2$value of zero, Tauc relation. The reported bandgap energy value for the NiOwas in the range of 3.4–3.8 eV which is in good agreement with our article.The optical constants which include the refractive index n, extinction coefficient k, the real εr, and imaginary εi parts of dielectric constants were determined from transmission and absorption spectra within the range (200-1000)nm. The refractive index spectrum for NiO film, Figure (8), was almost constant at range(280-

1000)nm wavelength range, and decreased with decreasing wavelength.Figure (9) shows the variation of extinction coefficient as a function of wavelength for NiO thin films. It is observed from this Figure that the extinction coefficient slightly changed at visible range. Also, it was observed from this figure that the extinction coefficient before 360 nm wavelength increasing highly with increased the wavelength opposite to the variation of the refractive index, but the less values of extinction at 360 nm. Figure (10, 11) shows the variation of real (Ɛr) and imaginary (Ɛi) dielectric constants for NiO thin films. One can observe that the variation of (Ɛr) has a similar trend to that of the refractive index because of the smaller value of K^2 in comparison with n^2, while the variation of (Ɛi) mainly depends on the K value, which is related to the variation of absorption coefficient (Ɛi) represent the absorption of radiation by free carriers. It is observed from the Figures that the real and imaginary dielectric constants increase with the increase of the wavelength of the incident radiation in range (300-360) nm and this behavior is due to the change of reflectance and absorbance., and constant after 360 nm. Figure (12) shows the photo luminescence response curve of the sample. The characteristics was examined by exciting the sample with incident light of energy (3.06) eV at 405 nm. The resulting emission characteristics showedtwo peaks, the first one around 405 nm and the other around 450 nm.

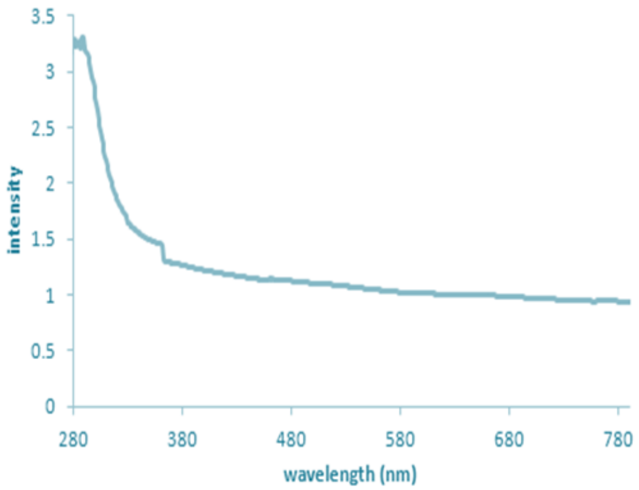

Figure 6: The optical absorbance of NiO thin films

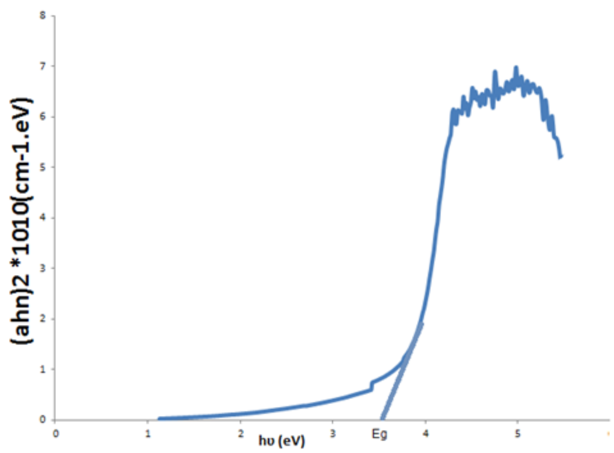

Figure 7: Variation of $(\alpha h\upsilon)^2$ versus hυ eV for NiO thin films.

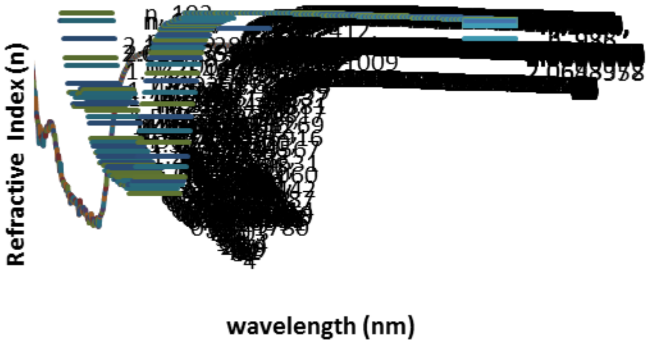

Figure 8: The Refractive Index(n) for NiO thin films at room temperature.

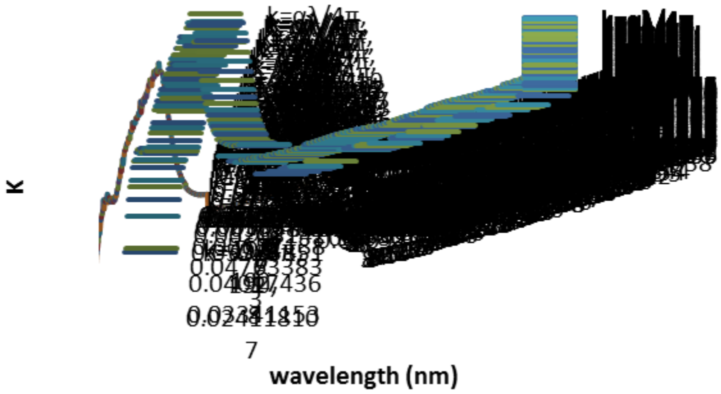

Figure 9:The Extinction coefficient for NiO thin films at room temperature.

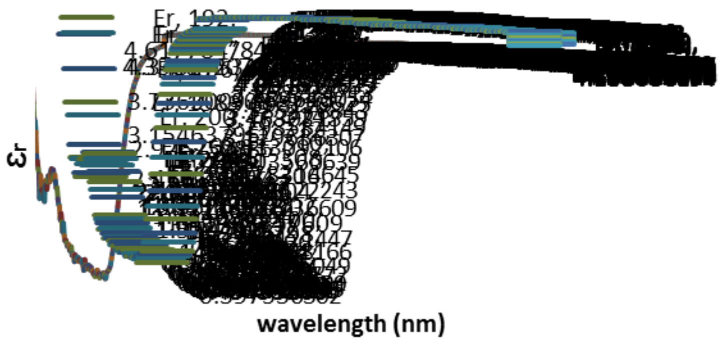

Figure 10: Real dielectric constant Ɛr for NiO thin films.

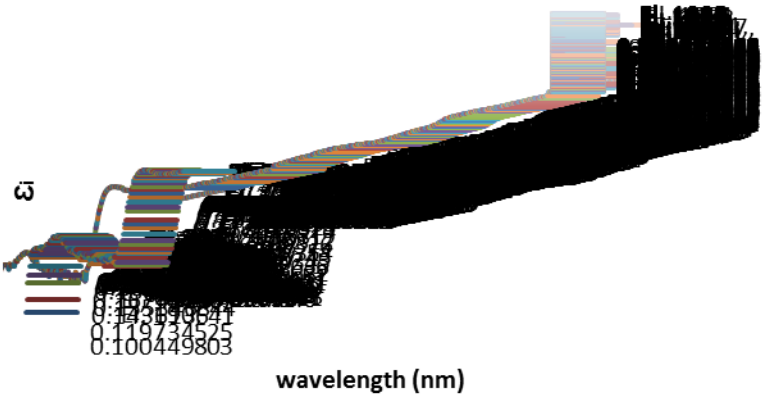

Figure 11: Imaginary dielectric constant Ɛi for NiO thin films

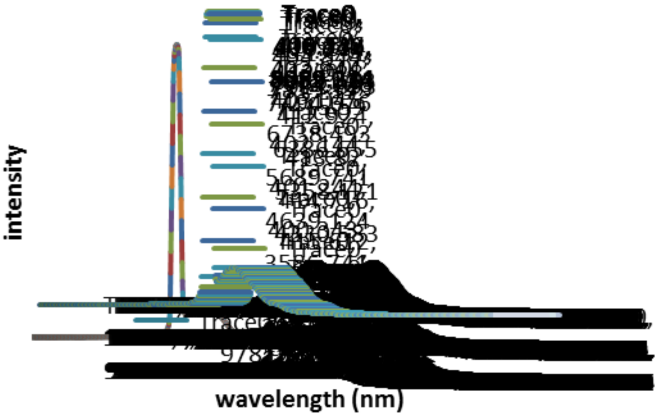

Figure 12: The fluorescence spectra for NiO thin films.

The conductivity type of the NiO thin film was determined by Hall coefficient (R_H) measurement at room temperature. The carrier concentration (n_H or p_H) and the Hall mobility (μ_H) were obtained from the combined Hall coefficient and electrical resistivity (ρ) measurement using the well-known equation:

$$n_H=1/e\,R_H \quad \text{and} \quad \mu_H=R_H/\rho \text{--------(2)}$$

The carrier concentration is given by the relation $n=r\,n_H$ where r (scatter factor) is usually assumed to be 1. Electrical resistivity of NiO thin films were studied by many researchers[20,21]and reported resistivity was in the range of $10 – 10^6$ Ω cm .Table 2 shows the Hall effect measurement data of NiOfilms.

Table 2: Hall effect measurement data.

Mobility μ_H	**103.2 cm2 /v.sec**	**Conductivity σ**	**1.939E-05(Ω.cm)$^{-1}$**
n $_H$	**1.2 (cm-3) * 10^{12}**	**type**	**P**

References

1. Cook JG, Koffyberg FP. (1984);Solar thermal absorbers employing oxides of Ni and Co. Solar Energy Materials. 10(1): 55-67.
2. Botejue Nadesan JC, Tseung ACC. (1985);Oxygen Evolution on Nickel Oxide Electrodes. Journal of the electrochemical society. 132(12): 2957-2959.
3. Koffyberg FP, Benko FA. (1981);p-Type NiO as a Photoelectrolysis Cathode. Journal of the electrochemical society. 128(11): 2476-2479.
4. Lampert CM. (1984);Electrochromic materials and devices for energy efficient windows. Solar Energy Materials. 11(1-2): 1-27.
5. C.A.Vincent, F. Bonion, M. Lizzari, B. Scrosati, Modern Batteries, 1sted,Edward Arnold, London,1987.
6. Bosman AJ, Crevecoeur C. (1966);Mechanism of the electrical conduction in li-doped NiO. Physical Review. 144(2): 763-770.
7. Tsu R, Esaki L, Ludeke R. (1969);Photoconductivity in Disordered Nickel-Oxide Films. Physical Review Letters. 23(17): 977-979.
8. Seike T, Nagai J. (1991);Electrochromism of 3d transition metal oxides. Solar Energy Materials. 22(2-3): 107-117.
9. Sato H, Minami T, Takata S, Yamada T. (1993);Transparent conducting p-type NiO thin films prepared by magnetron sputtering. Thin Solid Films. 236(1-2): 27-31.
10. Hotový I, Búc D, Haščík Š, Nennewitz O. (1998);Characterization of NiO thin films deposited by reactive sputtering. Vacuum. 50(1-2): 41-44.
11. Lampert CM, Omstead TR, Yu PC. (1986);Chemical and optical properties of electrochromic nickel oxide films. Solar Energy Materials. 14(3-5): 161-174.
12. Pramanik P, Bhattacharya S. (1990);A Chemical Method for the Deposition of Nickel Oxide Thin Films. Journal of the electrochemical society. 137(12): 3869-3870.
13. Varkey AJ, Fort AF. (1993);Solution growth technique for deposition of nickel oxide thin films. Thin Solid Films. 235(1-2): 47-50.
14. Chigane M, Ishikawa M. (1998);XRD and XPS characterization of electrochromic nickel oxide thin films prepared by electrolysis-chemical deposition. Journal of the Chemical Society - Faraday Transactions. 94(24): 3665-3670.
15. Utriainen M, Kröger-Laukkanen M, Niinistö L. (1998);Studies of NiO thin film formation by atomic layer epitaxy. Materials Science and Engineering B. B54(1-2): 98-103.
16. Surca A, Orel B, Pihlar B, Bukovec P. (1996);Optical, spectroelectrochemical and structural properties of sol-gel derived Ni-oxide electrochromic film. Journal of Electroanalytical Chemistry. 408(1-2): 83-100.
17. Camelia MATEI GHIMBEU, "Preparation and Characterization of metal oxide semiconductor thin films for the detection of atmospheric pollutant gases", University Paul Verlaine of Metz, France, Ph. D. Thesis, 2007.
18. Jaworek A, Krupa A. (1999);Classification of the modes of EHD spraying. Journal of Aerosol Science. 30(7): 873-893.
19. Shi J, Zhu Y, Zhang X, Baeyens WRG, Garcĺa-Campaĺ±a AM. (2004);Recent developments in nanomaterial optical sensors. TrAC - Trends in Analytical Chemistry. 23(5): 351-360
20. Ando M, Sato Y, Tamura S, Kobayashi T. (1999);Optical humidity sensitivity of plasma-oxidized nickel oxide films. Solid State Ionics. 121(1): 307-311.
21. Sato H, Minami T, Takata S, Yamada T. (1993);Transparent conducting p-type NiO thin films prepared by magnetron sputtering. Thin Solid Films. 236(1-2): 27-31.

*****